

New Developments in Shrouds and Augmentors for Subsonic Propulsion Systems

Michael, J. Werle, PhD¹
FloDesign Inc., Wilbraham, MA 01095

and

Walter M. Presz, Jr., PhD²
Western New England College and FloDesign Inc., Wilbraham, MA 01095

A new, simple and handy control volume formulation is put forward for propellers in shrouded installations with ejector-augmented systems. It is first-principles based, free of empiricisms, overcomes past formulation limitations and uncovers here-to-fore unknown high thrust potential for such systems. The control volume predictions agree well with both existing experimental and computational data for shrouded propellers, and other analytical and empirical models. Solutions involve simple polynomials (closed form expressions for shrouded propellers) with a single input parameter related to the aerodynamics of the empty shroud. This formulation provides new correlation parameters, plus greatly simplifies design optimization studies by decoupling the shroud design effort from that of the propeller design.

I. Introduction

For the analysis and/or design of shrouded propeller systems as depicted in Figure 1, a mature literature has evolved over the past 100 years for both aeronautical and marine applications. These are largely based on either empirical correlations or tedious and/or complex analytical/computational modeling of flow involving ringed airfoils (see Refs 1-9 for example). As such, they are found to be difficult to employ when exploring wide ranges of geometric influences and/or conducting design optimization studies.

Similarly, while ejector-based propulsion augmentation has been studied extensively for over 60 years (see Refs 10-16 for examples), only limited attention has been given its application to subsonic/incompressible prop systems. Literally hundreds, if not thousands, of papers, articles, reports and books have discussed ejector based thrust augmentation at length for configurations such as depicted in Figure 2 involving the interaction of primary and secondary streams that are fluid-dynamically independent. Two key papers on the subject are those of Von Karman (Ref. 10 and as discussed in Ref. 1 for example) and Heiser (Ref. 11). Von Karman introduced the simple one dimensional momentum balance model of Figure 2 to predict the amplification of an independent primary jet's thrust due to ingestion of free stream fluid into a constant area duct that exhausts downstream to the free stream's far field pressure level. All efforts since that time have employed this same basic model, which contains the two critical assumptions/constraints: (1) an independent primary stream ingesting free stream fluid through an ejector opening and (2) the combined (mixed) flow exiting the ejector at the free stream pressure level. These two assumptions are inappropriate for low-speed and/or incompressible flow for shrouded propeller systems such as depicted in Figure 3. The system shown has power added or extracted from the primary stream, and flow circulation associated with each shroud. For this case, the primary stream must be accounted for as a portion of the free stream that has been modified due to the power injection or extraction and the free stream pressure must be imposed far downstream of the ejector exit.

¹ Chief Scientist, 390 Main Street, Wilbraham, MA 01095, AIAA Fellow

² Emeritus Professor of Mechanical Engineering and Chief Technology Officer, 390 Main Street, Wilbraham, MA 01095, AIAA Member

The current study extends the shrouded prop system formulation introduced by the present authors in Ref. 17 to include an ejector-augmentor incorporated into the shroud system. As depicted in Figure 3 for a one-stage ejector, in this case, the entire system is strongly coupled such that the ejector-augmentor affects the primary flow and vice versa. The simple one dimensional, first-principles base, analytical model, free of empirical constants, first developed in Ref. 17 has been extended to include both one and two stage ejectors augmentors. Only the single-stage results will be discussed herein while the two-stage analysis, which is a straightforward but rather tedious extension of that presented here and Ref. 18, will be the subject of a future paper.

The unified formulation for shrouded and augmented prop-based systems provided here is both new and tedious. It is therefore presented below in step-wise fashion—first by introducing, solidifying and verifying basic concepts for the shrouded case in Section II and thereafter extending the formulation to the case of a one-stage ejector-augmentor in Section III. Sample results are then presented, as well verifying comparisons with other solutions and data for shrouded props. Finally, a compendium of ejector-augmentor results is presented for study, analysis and design guidance.

II. New Formulation of Governing Eq.s for Shrouded Props

Figure 1 provides the geometry and nomenclature applied here. The current formulation employs a key element that differentiates it from previous works: a novel explicit incorporation into the formulation of the shroud produced axial force, F_S , of Figure 1 to appropriately account for the flow effects associated with any circulation/energy exchange interaction.

With regard to F_S , it is useful to first review the flow physics attendant to the shrouded prop systems. As discussed in Ref. 1 for example, in the shrouded flow depicted in Figure 4, any axial pressure change due to, for example, a prop causes the flow streamlines upstream and downstream to expand or contract laterally, giving rise to a velocity component normal to the shroud. Because of this, the Kutta-Jackowski theorem then requires that its interaction with the ring vortex vector associated with the duct's circulation produces an axial force, F_S . The critical aspect of this model is that it relates the axial force on the shroud solely and directly to the force on the fluid caused by the axial change in the pressure. From this and dimensional analysis considerations, the current formulation sets the shroud axial force (see Figure 1 for nomenclature) as being proportional to the prop induced force through a shroud coefficient, C_S , as:

$$F_S = A_p (p_{p2} - p_{p1}) C_S \quad (1)$$

which, with Bernoulli's equation, becomes:

$$F_S = \frac{1}{2} [\rho A_p (V_o^2 - V_a^2)] C_S \quad (2)$$

An overall momentum, mass and energy balance is then applied to the flow structure and the cut of Figure 5 for a finite wind-tunnel like flow cross-sectional area, A_T , which is then allowed to become infinite as the cut around the shroud shrinks to the shroud outline, yielding:

$$\frac{1}{2} (1 + C_S) (V_o^2 - V_a^2) = V_p (V_o - V_a) \quad (3)$$

The resulting velocity flowing through the prop is then given as:

$$V_p = \frac{1}{2} (1 + C_S) (V_o + V_a) \quad (4)$$

and the power injected/extracted from the flow is given by:

$$P = \frac{1}{4} \rho A_p (1 + C_s) (V_o + V_a) (V_o^2 - V_a^2) \quad (5)$$

The total thrust produced is than given as:

$$T = (1 + C_s) P / V_p = 2P / (V_o + V_a) \quad (6)$$

and the thrust on the prop is given as

$$T_p = P / V_p = T / (1 + C_s). \quad (7)$$

The formulation provided in Equations 1-7 applies equally to all shrouded prop-based systems, either propulsors or power generators. Only the former will be discussed here with the latter presented in detail in Refs. 17 and 18.

For the propulsor case, this equation set demands a choice be made of the principle independent variable. This choice depends on which is most appropriate to the situation: either (1) the power through the propeller to the flow field, (2) the total pressure rise induced by the propeller or (3) the static pressure at the primary duct exit, A_p , of Figure 1. Options 2 and 3 are the most straightforward (and a bit simpler algebraically) but option 1 is the focus of the current formulation so as to allow detailed assessment of the thrust output potential for fixed input power levels. For this case Equations 3 through 5 can be combined to write that:

$$v_o^3 + v_a v_o^2 + v_a^2 v_o - 1 - v_a^3 = 0 \quad (8)$$

where use has been made of the following definitions:

$$V_c \equiv V_p / (1 + C_s)^{1/3} \quad (9)$$

$$V_p \equiv (4P / \rho A_p)^{1/3} \quad (10)$$

$$v_o \equiv V_o / V_c \quad v_p \equiv V_p / V_c \quad v_a \equiv V_a / V_c \quad (11)$$

Note the ‘‘Power’’ velocity, V_p , of Equation 10 is closely related to the disk loading coefficient used by others, e.g., Ref. 1.

The exact solution to the cubic Equation 8 is given as

$$v_o = (1/2)^{1/3} \left[1 + 16/27 v_a^3 + \sqrt{1 - 32/27 v_a^3} \right]^{1/3} + (1/2)^{1/3} \left[1 + 16/27 v_a^3 - \sqrt{1 - 32/27 v_a^3} \right]^{1/3} - v_a / 3 \quad (12)$$

which can be approximated using a Taylor series as:

$$v_o \approx 1 - 1/3 v_a + 4/9 v_a^2 \quad (13)$$

These in turn can be used in Equation 6 to calculate the shrouded systems total thrust in terms of a new thrust coefficient defined as:

$$C_{TP} \equiv \frac{T}{\frac{1}{2}\rho A_p V_P^2} = (1 + C_S)^{1/3} / (v_a + v_o) \approx (1 + C_S)^{1/3} / \left(1 + \frac{2}{3}v_a + \frac{4}{9}v_a^2\right) \quad (14)$$

At this point it is worth pausing to take note of some of the rather profound aspects of the above results. To the degree that the newly introduced shroud force coefficient formulation defined in Equation 1 is valid (as discussed later):

- We now have at hand the solution of the entire shrouded prop problem reduced to simple polynomial relations with a single input parameter, the shroud coefficient, C_S .
- The unshrouded (bare) prop case is recovered setting $C_S = 0$ (giving $C_{TP} = 1$) as but one of an infinite and continuous family of solutions dependent solely on C_S .
- Most importantly, C_S can be very easily determined by applying Equation 4 at the zero power state, i.e., the empty shroud in a uniform free stream, to write that:

$$\left(\frac{V_p}{V_a}\right)_{P=0} = 1 + C_S \quad \text{or} \quad C_S = \left(\frac{V_p}{V_a}\right)_{P=0} - 1 \quad (15a)$$

which states that the shroud coefficient can be determined directly from the free stream induced velocity at the prop station when no prop is present.

- Equation 14 defines the maximum thrust one can ever generate for any prop system (shrouded or not) for a given power loading. It's value occurs with zero forward velocity and is given by:

$$\left(C_{TP}\right)_{\max} = \left(\frac{V_p}{V_a}\right)_{P=0}^{1/3} \quad (15b)$$

- Design and optimization studies can now be greatly simplified because this formulation leads to a handy decoupling of the shroud design effort from the prop system design for any power level. The challenge now is to design a family of shrouded prop systems that minimize losses due to viscosity, tip leakage, swirl, etc. so as to maximize C_S at $P=0$.

This new formulation can be related to earlier formulations by first noting that the shroud exit pressure level can be written as;

$$C_{pPD} \equiv \frac{P_D - p_a}{\frac{1}{2}\rho V_P^2} = \left(v_a^2 + 1/(v_a + v_o) + \left[\frac{1}{2}(1 + C_S)A_p/A_D \right]^2 \right) / (1 + C_S)^{2/3}, \quad (16a)$$

which can be related to the static case thrust level (at $V_a=0$) using the approximate form of Equation 14 and further Taylor series approximations to write that:

$$C_{TP0} \equiv \left(C_{TP}\right)_{V_a=0} = (1 + C_S)^{1/3} \approx \left(2A_{Dp}\right)^{1/3} - A_{Dp}C_{pPD}. \quad (16b)$$

Equation 16b shows that the static thrust is related to the shroud exit pressure and diffusion levels, which themselves are interdependent and uniquely related to the shroud coefficient, C_S . It will also be employed later in comparisons with the static thrust correlations and data of Refs. 3 and 4 and can be further exploited by combining Equations 14 & 16, leading to:

$$C_{TP}/C_{TP0} \approx 1 / \left(1 + \frac{2}{3}v_a + \frac{4}{9}v_a^2\right) = 1 / \left(1 + \frac{2}{3}C_{TP0} \frac{V_a}{V_P} + \frac{4}{9}C_{TP0}^2 \frac{V_a^2}{V_P^2}\right) \quad (17a)$$

It is noted in passing that the independent variable in Equation 17a can also be written as a generalization of that given by McCormick (Ref 1) and others as:

$$C_{TP0} V_a / V_P = V_a / \sqrt{T_0 / 2(1 + C_S) \rho A_p} \quad (17b)$$

Equation 17a provides not only a simple closed form polynomial solution for the thrust, but also identifies two correlation parameter, C_{TP}/C_{TP0} and $C_{TP0}(V_a/V_P)$ which applies to all unshrouded and shrouded props.

III. Governing Equations for One-Stage Ejector Augmentors

To extend the shrouded prop formulation of Section 2 to that of the ejector-augmentor depicted in Figures 3 & 6, it is first necessary to take note that the ejector duct always gives rise to a pressure increase caused by the mixing of the primary and secondary streams. This can be shown by applying a one dimensional momentum balance to the constant area mixing region to find that:

$$p_d - p_s = \rho(A_s/A_d) [(V_D - V_s)/(A_D + A_s)]^2 \quad (18)$$

Thus for a shrouded prop plus ejector, the total axial force induced on the fluid is found to have two components; one that is a result of the pressure change across the prop discussed in Section 2, and one that is a result of the pressure increase in the ejector duct. With Equation 18, and following the logic of Equation 1 in Section 2, the force on the two shroud elements is again taken to be linearly related to the axial pressure forces through the shroud axial force coefficient, C_S , as:

$$F_S \equiv F_{S1} + F_{S2} = \{A_p(p_{p2} - p_{p1}) + A_d(p_d - p_s)\} C_S, \quad (19)$$

which, with the use of Bernoulli's equation becomes:

$$F_S = \left\{ \frac{1}{2} \rho A_p (V_D^2 - V_s^2) + \rho A_D (V_D - V_s)^2 r_s / (1 + r_s) \right\} C_S. \quad (20)$$

Here r_s is introduced as the ratio of the ejector duct inlet area, A_s , to the primary duct diameter, A_D such that:

$$A_d = A_D + A_s = (1 + r_s) A_D. \quad (21)$$

Similar to the shrouded prop case of Section 2 and Figure 5, an overall momentum, mass and energy balance can be applied to the flow structure and the cut of Figure 7 for a finite wind-tunnel like flow cross-sectional area, A_T , which again is than allowed to become infinite as the cuts around the two shroud elements shrink to the shroud outlines to yield:

$$aV_D^2 - bV_s^2 - 2r_s C_S V_s V_D = (1 + r_s)(V_D + r_s V_s)(V_0 - V_a) \quad (22a)$$

where:

$$a \equiv \frac{1}{2} A_p / A_D (1 + C_S)(1 + r_s) + r_s C_S \quad (22b)$$

and

$$b \equiv \frac{1}{2} A_p / A_D (1 + C_s) (1 + r_s) - r_s C_s. \quad (22c)$$

The power introduced (or extracted) can be related to the primary and secondary stream velocities as:

$$P = \frac{1}{2} \rho A_D V_D (V_D^2 - V_S^2) \quad (23)$$

To complete the formulation, flow through the ejector duct of Figure 6 can be related to the free stream conditions using the Bernoulli and the continuity equations to write:

$$(V_S + r_s V_D)^2 = (1 + r_s)^2 (V_D^2 + V_a^2 - V_O^2). \quad (24)$$

As before, Equations 19-24 apply equally to either thrust generation due positive power input or power extraction, with the former discussed in detail below and the latter presented in Ref. 18.

The governing equations are non-dimensionalized as in Section 2 (i.e., with the power as an independent variable) using the definitions of Equations 9-11 to write that:

$$a v_D^2 - b v_S^2 - 2 r_s C_s v_S v_D = (1 + r_s) (v_D + r_s v_S) (v_O - v_a), \quad (25)$$

$$(v_S + r_s v_D)^2 = (1 + r_s)^2 (v_D^2 + v_a^2 - v_O^2), \quad (26)$$

$$v_D (v_D^2 - v_S^2) = \frac{1}{2} (1 + C_s) A_p / A_D. \quad (27)$$

For given values of the shroud coefficient, C_s , the area ratios, A_E/A_d , A_D/A_p , A_E/A_p and the forward velocity, v_a , Equations 25-27 form a closed set and can be solved (iteratively) for v_D , v_S , and v_O . With these values in hand, it is straightforward to calculate the output parameters of interest:

$$\text{Total Thrust:} \quad C_{TP} \equiv T / \left(\frac{1}{2} \rho A_p V_P^2 \right) = 2 A_D / A_p (v_D + r_s v_S) (v_O - v_a) / (1 + C_s)^{2/3}, \quad (28)$$

$$\text{Prop Thrust:} \quad C_{TPp} \equiv T_p / \left(\frac{1}{2} \rho A_p V_P^2 \right) = (v_D^2 - v_S^2) / (1 + C_s)^{2/3}, \quad (29)$$

$$\text{Exit Pressure:} \quad C_{pPE} \equiv (p_E - p_a) / \left(\frac{1}{2} \rho V_P^2 \right) = \left\{ v_O^2 - \left[A_d / A_E (v_D + r_s v_S) / (1 + r_s) \right]^2 \right\} / (1 + C_s)^{2/3}. \quad (30)$$

Similar to the shrouded prop system, Equation 28 gives the maximum thrust achievable from the ejector augmentor for any given power loading. Additionally, one can show that the applicable value of C_s can again be calculated from Equation 15b, i.e., for the uniform flow through the ejector shroud system of Figure 3 with no prop present. This again handily decouples the shroud and prop system design efforts.

IV. Results

Because the formulation and analyses presented above are new and different, it is appropriate to now provide a representative range of predictions for inspection plus provide evidence of their validity through comparisons with experimental data and other analytical or empirical models, where available, for shrouded prop systems.

Attention will first be given to the shrouded (and bare) prop case predictions in order to set benchmarks for later assessing the ejector's influence. As indicated earlier, the bare prop case for static flight ($C_{TP} = 1$), recovered at $C_S=0$, is shown in Figure 8 to be but one of an infinite family of cases, all of which are also seem to be well represented by the simple polynomial approximation version of Equation 14 for both static and forward flight conditions.

Focusing first on the static flight case, Figure 9 shows the same results as Figure 8 but in terms of the shroud diffusion and exit pressure levels as discussed relative to Equation 16b. Here it is seen that: (a) thrust increases of nearly 80% above the bare prop level are attainable with moderate diffusion and exit plane suction pressures and (b) the handy approximation of Equations 13 & 14 gives a good representation over the regimes of interest. Note we have limited the shroud diffusion levels in this study to $A_D/A_p < 1.3$ because higher levels give rise to higher losses, more weight and longer length.

Figure 10 focuses on the forward flight velocity effects of Figure 8, showing the classic drop in the shroud's effectiveness to generate thrust augmentation as V_a increases. Again, the utility of the polynomial approximation of Equations 13 and 14 is apparent for both the bare and the entire family of shrouded prop cases. Most importantly, these same results are shown in Figure 11 to: a) collapse to a single curve including both the shrouded and unshrouded (bare) prop cases and b) further verify the utility of the Equation 13 approximation to the exact solution for virtually all values of forward velocity for all bare and shrouded props.

Turning now to verification of the control volume formulation, Figures 12 and 14 provide comparisons with the experimental/computational data as well as analytical and empirical predictions.

Attention is first given to the current models ability to predict the static thrust levels, C_{TP0} . To this end, Equation 16b has been used for comparisons with the data and empirical predictions of Refs. 3 and 4, which are presented in terms of a thrust-to-power ratio and diameter/disc-loading parameter as shown in Figure 12 for a very wide range of configurations—from air cushion machines to helicopters. Using Equations 14 and 16b, the current formulation predicts that for air one obtains the following thrust to power relationship:

$$T / P_{iH} = 0.85(1 + C_S)^{1/3} \left[D_p \sqrt{1000/P_{iH}} \right]^{2/3}, \quad (30a)$$

where use has been made of a prop efficiency ratio of 0.75 as proposed in Ref. 3. For the bare prop case where $C_S=0$, the prediction of Equation 30a is found to reproduce those provided in Refs 3 and 4 plus compare well with the data of Figure 12. Additionally, for a shrouded prop with an area ratio of 1 and zero exit pressure coefficient, Equation 16b gives $C_S=1$ so that Equation 30a now becomes:

$$T / P_{iH} = 1.08(1 + C_S)^{1/3} \left[D_p \sqrt{1000/P_{iH}} \right]^{2/3}. \quad (30b)$$

Equation 30b is found to exactly reproduce the correlation expressions of Refs. 3 and 4 plus again is seen in Figure 12 to well represent the shrouded data and trends. It is also found that for a shroud area ratio of 2, the prediction of Equation 30a using Equation 16b again reproduces the empirical expression of Ref. 4. As such, all these results further verify the current formulation's ability to represent the static thrust levels of bare and shrouded prop systems.

Turning attention now to forward flight effects, Van Manen & Superine (Ref. 5) provide an extensive data base for shrouded props as used in ship propulsors. Variations in shroud geometries were studied over a wide range of prop advance ratios and loadings for a fixed rotor speed. The measured thrust levels for two of the shrouds, designated N7 and N18, are provided in Figures 13 a and b in two forms. Results for two additional geometries were also provided in Ref. 5 but were found to fall between those presented in Figure 13 and thus added little to the verification process. Also shown are the experimental and computational (CFD) results of Bulten and van Esch as presented in Ref. 6. For all the cases shown, the data was presented as families of smooth continuous curves, not discrete data points. Thus one cannot be sure of the range of experimental variation in the measured results. For current purposes, the data has been marked here with discrete symbols at each advance ratio for identification purposes only.

As discussed in Ref. 18, converting the data of Refs. 5 and 6 to the current variables requires determination of the power being injected into the fluid by the prop. While it is known to be some percentage of the measured prop shaft torque multiplied by the rotor speed, the precise value was not explicitly stated in either Refs. 5 or 6. Thus for present purposes, the prop efficiency factor was determined two ways. The first of these employed a separate analysis of the Ref. 5 data set indicating values ranging from 0.71 to 0.85 depending on the nozzle and advance ratio. These were determined by making use of the approximation recommended by Van Manen & Superine for estimating the velocity at the prop station—which was not measured directly but rather inferred from separate tests. This approximation, apparently originally due to Froude, assumes that the prop advance ratio in the shroud is the same as that in a cylinder at the same level of the non-dimensionalized thrust. With this and the measured nozzle and prop thrust plus torque data, one can directly calculate a prop efficiency and thereafter the parameters of the current formulation. As shown in Figure 14a, quite remarkably, this causes all the data presented in Figure 13b to collapse to a single set. Further, the results are seen to necessarily lie below but closely track the current maximum thrust prediction over the full range of forward velocities—thus providing a strong endorsement of the current theoretical formulation and the utility of the correlation/scaling parameters it provides.

However, a level of uncertainty exists in the method described above for calculating prop efficiencies due to the fact it is expected that the prop's radial flow distributions between the two cases used in the Froude methodology would likely differ. Thus a second method was used which simply picked a value that best aligned the data with the predictions, in this case a value of 0.65. This level of prop efficiency is seen in Figure 14b to shift the entire data set virtually on top of the current model predictions.

Also shown in Figure 14 are the analytical predictions provided by McCormick (Ref. 1) for the N18 configuration. These were obtained using the scheme developed by Wessinger (Ref. 2) wherein the prop's influence on the circulation about the shroud, which is modeled as a single ring vortex, is approximated by a set of calculations involving tables and charts of tabulated results. To include the results of Ref. 1 in Figure 14 requires knowledge of the solution at $V_a=0$ in order to determine C_{TP0} , which was not provided. For current purposes, it was assumed that Equation 17a was valid between $V_a=0$ and the lowest value of V_a provided by Ref. 1, which in the current terms was found to be at $V_a/V_c=0.2$. This approach guarantees that McCormick's curve intersects the current solution at that point. Quite pleasingly, it is seen that thereafter the two results are virtually the same for all velocities, further highlighting and verifying the general utility of the current formulation and its attendant correlation parameters.

As a final note relative to verification of the current formulation, additional favorable comparisons with CFD predictions and experimental data are presented in Ref. 18 for two cases where power is extracted from the flow.

Turning attention now to the ejector-augmentor cases, Figures 15-17 provide results of a series of calculations for values of C_s from 1 to 3, ejector-augmentor area ratios from 1 to 5 at $V_a=0$. It can be shown that ejector-augmentor configurations with C_s values less than one do not have sufficient suction at the ejector port when r_s is small for flow to enter the ejector and thus are not considered further here. Note also that only 30% diffusion cases were considered here where $r_s = 0$ at $A_E/A_p=1.3$. In all cases, the solutions shown in Figures 15-17 for $r_s = 0$ reproduce the shrouded prop results provided in Figures 8 and 9, for which the thrust levels vary only with C_s per Equation 16b.

It is enlightening to first consider in detail the case of $C_s=1$ and zero diffusion, where it is noted in Figure 15 that the exit plane pressure coefficient is exactly zero for all ejector areas, A_E/A_p . This case is then seen to be the current equivalent of the traditionally provided solution (see Refs. 1, 10 and 11 for examples) wherein the pressure at the exit is imposed at the free stream level. Figure 16 shows that for this case the ejector can provide thrust augmentation levels of 25%-70% above that of the bare prop. More important, it is observed that higher values of C_s introduce an entirely new family of ejector solutions with significantly higher—double or more—thrust augmentation levels achievable over the bare propeller cases for the same input power. Note also, as indicated in Figure 15, the exit pressure level is only minimally influenced by the shrouds exit area diffusion level, whereas Figure 16 indicates a loss in augmentation for these cases.

A major benefit of ejector augmentors is indicated in Figures 17, showing that they shift the bulk of the new thrust generated from the prop to the shroud, i.e., from the rotating to the static structure of the system. Values significantly lower than the traditionally reported 50% level are seen to be obtainable for higher C_s and/or ejector

sizes. Thus the ejector system is seemed to be producing significantly more thrust at the same power levels through a structurally more robust configuration.

Finally, in Figs. 18 and 19 the influence of forward flight velocity on the ejector system's thrust augmentation compared to that of its bare prop equivalence is shown for a bare prop, a shrouded prop with $C_S = 3$ and an ejector-augmentor with $C_S = 3$ and $A_E/A_p = 3$. While in Fig 18 all show the expected decline with forward velocity, the ejector augmentor is seen to add significant thrust augmentation well above the bare and shrouded prop equivalents, even at relatively high forward flight speeds. Figure 19 displays the same results but in terms of the propeller efficiency levels. While the ejector augmentor is seen to always have efficiencies above those of the bare and even shrouded prop, most notable is the large gain at lower velocities and/or higher disc loading levels. At lower velocities with higher disc loading, gains of over 100% are seen to be possible in terms of prop efficiencies.

V. Concluding Remarks

As simple as the above formulation is, it is hard to overstate the importance of its implications or its utility for shrouded and/or ejector augmented systems.

First, the unified and empirically free analyses presented for shrouded prop systems was verified through comparisons with experimental and computational data, plus other appropriate analytical and empirical models. The results definitively established that:

- A practical, control volume solution of an entire shrouded prop and ejector augmentor system is now at hand and is reduced to simple polynomial relations with a single input parameter, the shroud coefficient, C_S .
- The formulation applies equally for power addition or extraction from the primary stream with flow circulation effects associated with each shroud.
- The unshrouded (bare) prop case is recovered as but one of an infinite and continuous family of solutions dependent solely on C_S .
- C_S can be very easily determined directly from the free stream induced velocity at the prop station when no prop is present.
- The solution defines the maximum thrust one can ever generate for any prop system (shrouded or not) for a given power loading which is given by:

$$\left(C_{TP}\right)_{\max} = \left(V_p/V_a\right)_{P=0}^{1/3}. \quad (31)$$

- Design and optimization studies can take advantage of the handy decoupling of the shroud design effort from the prop system design for a specific power level to be injected by the prop
- A properly designed shrouded propeller and ejector augmentor system has the potential to dramatically increase the thrust generation capabilities of props.
- A family of shrouded prop systems now have to be designed with high circulation and low losses to take advantage of the new thrust potential identified.

It was also highlighted, that the shroud exit pressure level is uniquely coupled to the shroud's diffusion level through the shroud axial force coefficient C_S . These cannot be set independently if the maximum performance is to be achieved. Additionally, this formulation has provided new set of correlation parameters for all shrouded and unshrouded prop systems. Most importantly, this formulation provides a straightforward algebraic design methodology (and path to optimization) for shrouded propulsors.

Finally, the control volume analyses presented herein definitively show that ejectors can deliver significant thrust augmentation to shrouded prop systems in low speed flows. These results are new and are the result directly from extension of the shrouded propeller formulation. The removal of unnecessary and incorrect boundary condition constraints at the shroud exit uncovered significant levels of thrust augmentation potential possible with ejectors—in some cases by a factor of two or more. This benefit over that of the shrouded and bare prop cases continued even as the forward flight velocity increased appreciably. Also, most significantly, it was found that while the ejector augmentors do generate added thrust, they also shift the bulk of that loading to the shroud, i.e., from the rotating to static structure. This should result in highly productive systems that are not only compact but structurally very

robust. The current formulation applied to the ejector augmentor system also leads to a decoupling of the shroud system design from that of the prop system, greatly simplifying design optimization studies.

References

1. McCormick, Barnes W. Jr., *Aerodynamics of V/STOL Flight*, Dover Publications, Minneola NY, 1999.
2. Weissinger, von Johannes, "Einige Ergebnisse aus der Theorie des Ring Fluegels in Inkompressibler Stromung", reprinted from *Advances in Aeronautical Sciences*, vol 2, Pergamom press, New York, 1959.
3. Marc de Piolenc, F., and Wright, G., *Ducted Fan Design*, Volume I, Millennial Year Edition, 2001, Mass Flow Publishing.
4. Department of Transportation, *Airworthiness Standards; Propellers*, Federal Aviation Regulation Part 35, Federal Aviation Administration, August 1974.
5. Van Manen, J.D. and Superine, A., "The Action of Screw Propellers in Nozzles", *International Shipbuilding Progress*, vol 6, No. 55, March 1959, pp 95-113.
6. Bulten, Norbet and van Esch, Bart, "Review of Thrust Prediction Method Based on Momentum Balance for Ducted Propellers and Waterjets", *Proceedings of the 2005 ASME Fluids Engineering Division Meeting*, June 19-23, 2005, Houston TX.
7. Stewart, H.J., "The Aerodynamics of a Ring Airfoil", *Quarterly Journal of Applied Mathematics*, Vol. 2, July 1944, pp137-141.
8. Mann, Michael J., "Subsonic Annular Wing Theory with Application to Flow About nacelles", NASA Technical Note TN D-760, September 1974.
9. Wagner, M.J., "Calculation of the Pressure Distribution and Streamline Pattern Around a Ring Wing Using Finite Difference Methods", AIAA Paper 83-0645, Presented at the AIAA 21st Aerospace Sciences Meeting, Reno, Nevada, January 10-13, 1983.
10. Von Karman, T., "theoretical Remarks on Thrust Augmentation", *Reissner Anniversary Vol., Contributions to Applied Mechanics*, J.W. Edwards Editor, Ann Arbor Michigan, 1949.
11. Heiser, William H., "Thrust Augmentation", ASME Paper #66-GT-116, 1966
12. Presz, Jr, W., Reynolds, G and Hunter, C: "Thrust Augmentation with Mixer/Ejector Systems", AIAA Paper # 2002-0230, presented at 40th AIAA Aerospace Sciences Meeting & Exhibit 14-17 January 2002 / Reno, NV
13. W. Presz, Jr. and M Werle, "Multi-stage Mixer Ejector Systems", American Institute of Aeronautics and Astronautics Paper # 2002-4064 presented at the 38th AIAA/ASME/SAE/ASEE joint Propulsion Conference and Exhibit, Indianapolis, IN, 7-10 July, 2002.
14. Quinn, Bryan, Compact "Ejector Thrust Augmentation", *Journal of Aircraft*, vol 10, No. 8 August 1973, pp 481-486
15. Kentfield, J.A.C., "The Prediction of the performance of Low Pressure-ratio Thrust-Augmentor Ejectors", AIAA Paper 78-145, presented at the AIAA 16th Aerospace Sciences meeting, Huntsville, AL, January 16-18, 1978
16. Porter, J.I. and Squyers, R.A., "An Overview of Ejector Theory", AIAA Paper 81-1678, presented at the AIAA Aircraft systems and Technology Conference, Dayton OH, August 11-13, 1981
17. Werle, M.J. and Presz, jr. W., "Ducted Wind/Water Turbines and Propellers Revisited", Technical note submitted to AIAA Journal of Propulsion and Power, June 2007.
18. Werle, M.J., and Presz Jr., W., "New Developments in Shrouds and Augmentors for Subsonic Power and Propulsion Systems", FloDesign Report FD 2007-10, March 23, 2007.

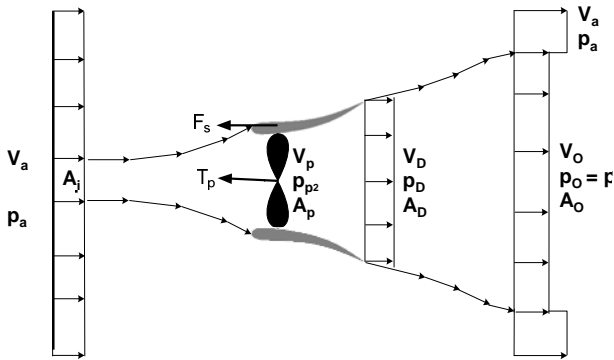


Figure 1: Shrouded System Nomenclature

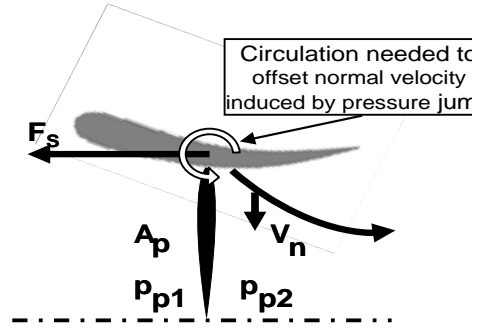


Figure 4. Axial Force Source

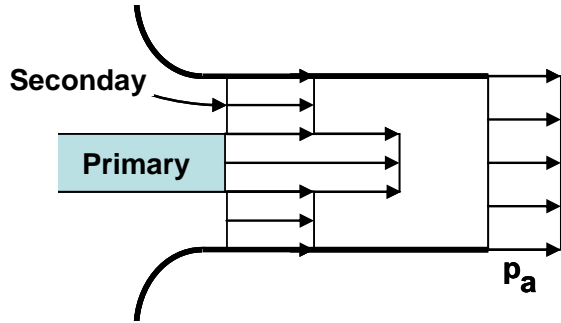


Figure 2: Traditional Ejector Model

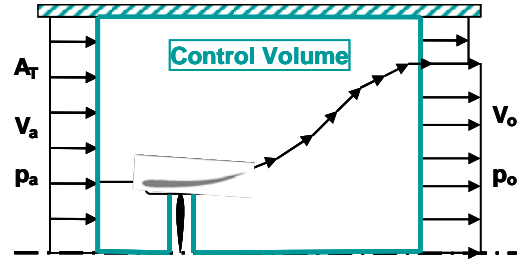


Figure 5. Control Volume Momentum Balance

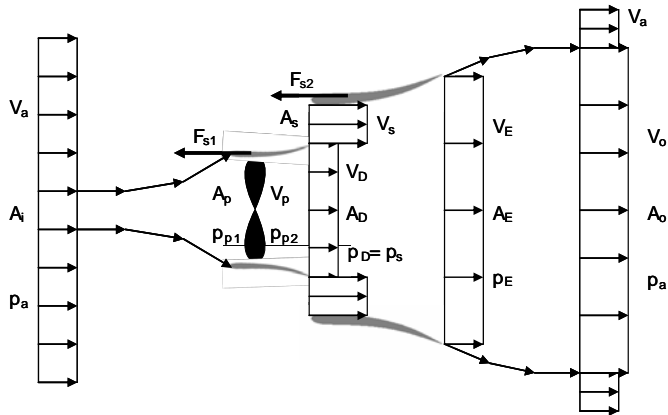


Figure 3. Ejector Augmentor Nomenclature

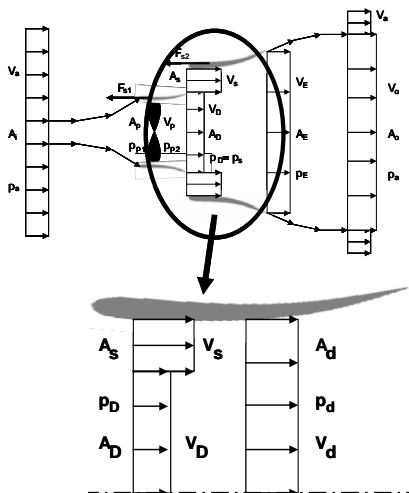


Figure 6. Ejector Mixing Model

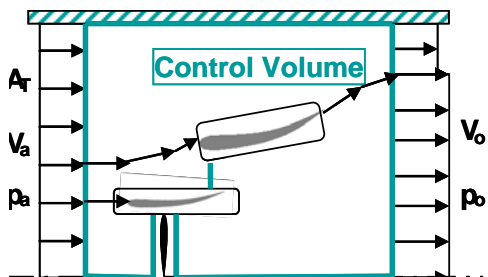


Figure 7: Ejector Control Volume

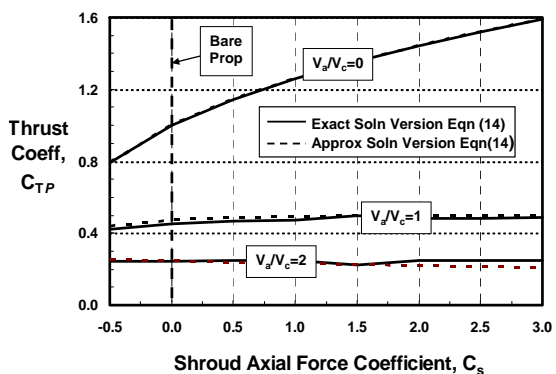


Figure 8. Velocity Effect on Shrouded Prop

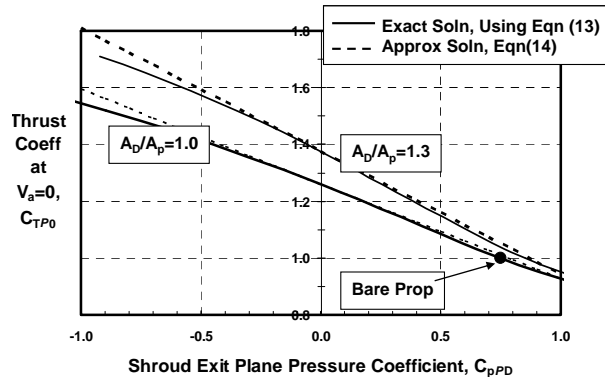


Figure 9: Shrouded Prop Performance at $V_a=0$

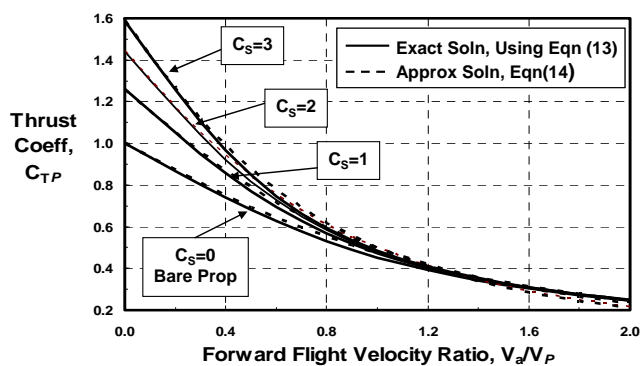


Figure 10. Forward Flight Influence on Thrust

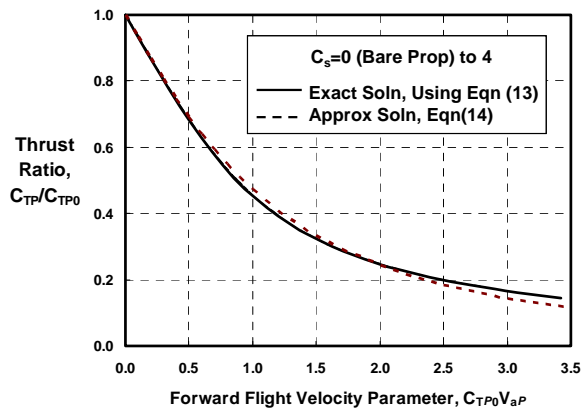


Figure 11. Shrouded Prop Thrust Correlation $V_a > 0$

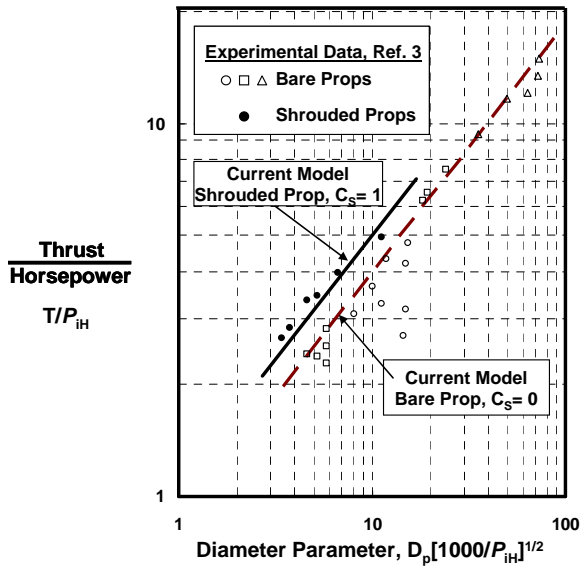
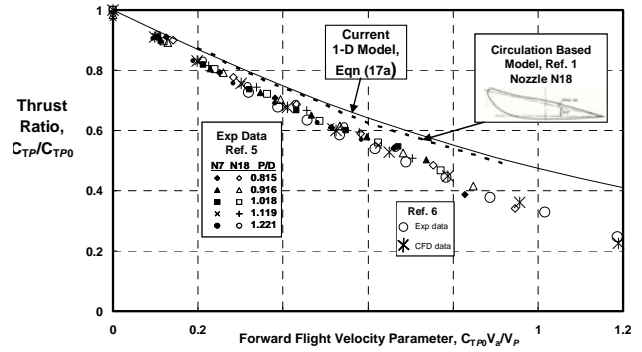
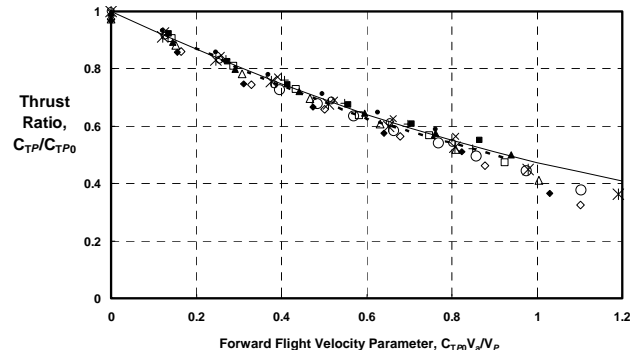


Figure 12. Bare & Shrouded Prop Static Thrust

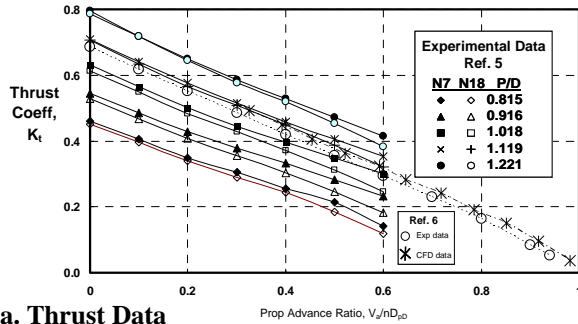


a. Data Inferred Prop Efficiencies

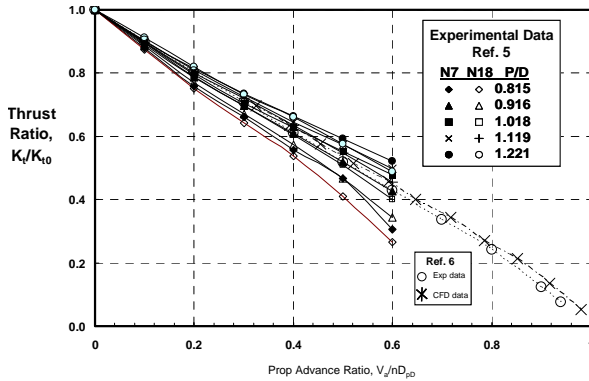


b. Estimated Prop Efficiencies = 0.65

Figure 14: Shrouded Prop Models/Data Correlations



a. Thrust Data



b. Thrust Ratio Data

Figure 13: Shrouded Propulsor Data

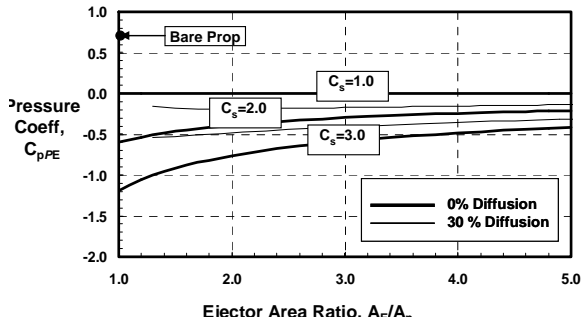


Figure 15. Ejector Exit Plane Pressure. $V_a=0$

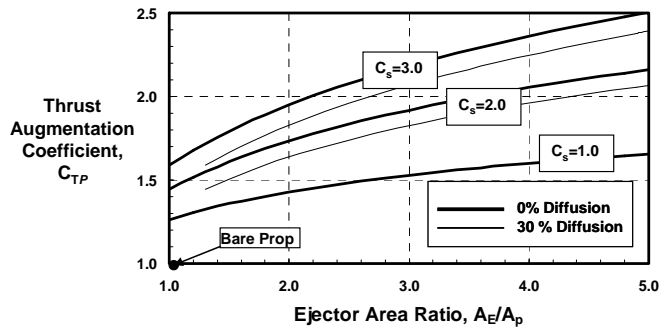


Figure 16. Ejector Thrust Augmentation. $V_a=0$

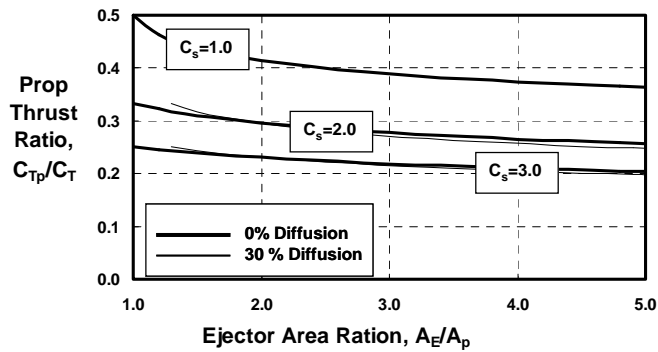


Figure 17. Ejector Augmentor Prop Thrust Levels, $V_a=0$

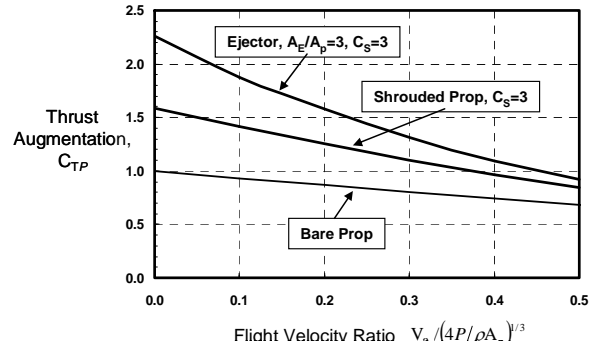


Figure 18. Ejector Forward Flight Influence

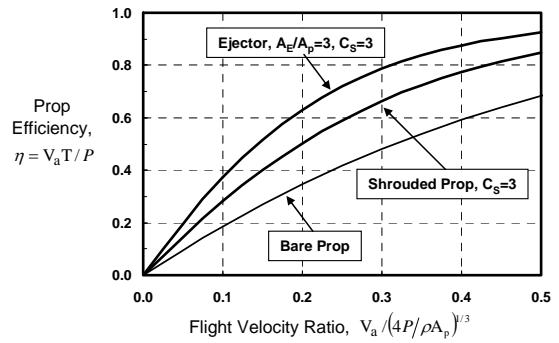


Figure 19. Ejector Propeller Efficiencies